AFRL-RY-WP-TP-2009-1304

EFFECT OF BANDWIDTH ON WIDEBAND-STAP PERFORMANCE (PREPRINT)

Ke Yong Li, Unnikrishna S. Pillai, and Joseph R. Guerci

C & P Technologies, Inc.

OCTOBER 2007

Approved for public release; distribution unlimited.

See additional restrictions described on inside pages

STINFO COPY

AIR FORCE RESEARCH LABORATORY
SENSORS DIRECTORATE
WRIGHT-PATTERSON AIR FORCE BASE, OH 45433-7320
AIR FORCE MATERIEL COMMAND
UNITED STATES AIR FORCE

REPORT DOCUMENTATION PAGE

Form Approved
OMB No. 0704-0188

1. REPORT DATE *(DD-MM-YY)*
October 2007

2. REPORT TYPE
Conference Paper Preprint

3. DATES COVERED *(From - To)*
25 May 2006 – 19 October 2007

4. TITLE AND SUBTITLE
EFFECT OF BANDWIDTH ON WIDEBAND-STAP PERFORMANCE (PREPRINT)

5a. CONTRACT NUMBER
FA8750-06-C-0117

5b. GRANT NUMBER

5c. PROGRAM ELEMENT NUMBER
62204F

6. AUTHOR(S)
Ke Yong Li (C & P Technologies, Inc.)
Unnikrishna S. Pillai (Polytechnic University)
Joseph R. Guerci (Guerci Consulting)

5d. PROJECT NUMBER
5017

5e. TASK NUMBER
RL

5f. WORK UNIT NUMBER
517R1511

7. PERFORMING ORGANIZATION NAME(S) AND ADDRESS(ES)
C & P Technologies, Inc.
317 Harrington Avenue
Suites 9 & 10
Closter, NJ 07624-1911

Polytechnic University
Brooklyn, NY 11201

Guerci Consulting
2209 North Utah Street
Arlington, VA 22207

8. PERFORMING ORGANIZATION REPORT NUMBER

9. SPONSORING/MONITORING AGENCY NAME(S) AND ADDRESS(ES)
Air Force Research Laboratory
Sensors Directorate
Wright-Patterson Air Force Base, OH 45433-7320
Air Force Materiel Command
United States Air Force

10. SPONSORING/MONITORING AGENCY ACRONYM(S)
AFRL/RYRT

11. SPONSORING/MONITORING AGENCY REPORT NUMBER(S)
AFRL-RY-WP-TP-2009-1304

12. DISTRIBUTION/AVAILABILITY STATEMENT
Approved for public release; distribution unlimited.

13. SUPPLEMENTARY NOTES
Conference paper to be published in the Proceedings of the 41st Annual Asilomar Conference on Signals, Systems, and Computers, held November 04 - 07, 2007 at the Asilomar Hotel and Conference Grounds, Pacific Grove, CA. PAO Case Number: WPAFB 07-0330; Clearance date: 05 Nov 2007. Paper contains color. See also, AFRL-RY-WP-TP-2009-1303 for a briefing chart version, and AFRL-RY-WP-TP-2009-1305 for a postprint version of the paper.

14. ABSTRACT
A wideband signal occupies a finite bandwidth that is significant compared to its carrier frequency. As a result, when transmitted, its returns cause bandwidth dispersion across the antenna. It is shown here that the effect of the finite bandwidth is to introduce a set of uncorrelated return signals for every physical scatter in the field. Further, each such uncorrelated return contains a set of coherent signals with different directional and Doppler components that result from a jittering effect both in angle and Doppler domain. As a result, adaptive clutter cancellation using traditional processing schemes does not work well. Although in principle it is possible to correct these decorrelating effects by 3D spacetime adaptive processing (STAP), the present day methods are quite costly and difficult to implement. In addition to the new wide band signal modeling framework mentioned above, we outline a hierarchical processing scheme which has the potential for dramatically reducing both processing and sample support burdens.

15. SUBJECT TERMS
wideband space-time adaptive processing

16. SECURITY CLASSIFICATION OF: a. REPORT	b. ABSTRACT	c. THIS PAGE	17. LIMITATION OF ABSTRACT:	18. NUMBER OF PAGES	19a. NAME OF RESPONSIBLE PERSON (Monitor)
Unclassified	Unclassified	Unclassified	SAR	10	Michael J. Callahan **19b. TELEPHONE NUMBER** *(Include Area Code)* N/A

Standard Form 298 (Rev. 8-98)
Prescribed by ANSI Std. Z39-18

Effect of Bandwidth on Wideband-STAP Performance

S. Unnikrishna Pillai[1], Ke Yong Li[2] and Joseph R. Guerci[3]

[1] Electrical Engineering Department, Polytechnic University, Brooklyn, NY 11201, pillai@hora.poly.edu
[2]C & P Technologies, Inc., Closter, NJ 07624, kli@cptnj.com
[3]Guerci Consulting, Arlington, VA, jrguerci@ieee.org

***Abstract*-A wideband signal occupies a finite bandwidth that is significant compared to its carrier frequency inasmuch as when transmitted, its returns cause bandwidth dispersion across the antenna. It is shown here that the effect of the finite bandwidth is to introduce a set of uncorrelated return signals for every physical scatter in the field. Further, each such uncorrelated return contains a set of coherent signals with different directional and Doppler components that result from a jittering effect both in angle and Doppler domain. As a result adaptive clutter cancellation using traditional processing schemes don't work well. Though in principle it is possible to correct these decorrelating effects by 3D space-time adaptive processing (STAP), the present day methods are quite costly and difficult to implement. In addition to the new wideband signal modeling framework mentioned above, we discuss a new hierarchical processing scheme which has the potential for dramatically reducing both processing and sample support burdens.**

I. INTRODUCTION

In the context of target detection in a wideband transmit/receive environment, consider an N element, M pulse array receiving signals from its field of view. In the narrowband setup with $e^{j\omega_o t}$ representing the transmit signal, after down converting to base band the array output space-time data vector $\mathbf{x}(t)$ from any range bin has the form

$$\mathbf{x}(t) = \sum_k \alpha_k \mathbf{s}(\theta_k, \omega_{d_k}) + \mathbf{n}(t) \tag{1}$$

where α_k represents the random scatter return from the k^{th} bin in the cross-range (azimuth) domain. Here

$$\mathbf{s}_k = \mathbf{s}(\theta_k, \omega_{d_k}) = \underline{b}(\omega_{d_k}) \otimes \underline{a}(\theta_k) \tag{2}$$

represents the $MN \times 1$ space-time steering vector with

$$\underline{a}(\theta_k) = \begin{bmatrix} 1 & e^{-j\omega_o \frac{d\sin\theta_k}{c}} & e^{-j\omega_o \frac{2d\sin\theta_k}{c}} & \cdots & e^{-j\omega_o \frac{(N-1)d\sin\theta_k}{c}} \end{bmatrix}^T \tag{3}$$

representing the spatial steering vector along θ_k and

$$\underline{b}(\omega_{d_k}) = \begin{bmatrix} 1 & e^{-j\pi\omega_{d_k}} & e^{-j2\pi\omega_{d_k}} & \cdots & e^{-j(M-1)\pi\omega_{d_k}} \end{bmatrix}^T \tag{4}$$

representing the temporal steering vector along the Doppler frequency

$$\omega_{d_k} = \frac{2VT\sin\theta_k}{\lambda/2}. \tag{5}$$

In (5), V represents the platform speed, T the pulse repetition interval and λ the operating wavelength.

In an uncorrelated clutter and noise scene, from (1), we get the space-time covariance matrix to be

$$\mathbf{R}_x = \sum P_k \mathbf{s}_k \mathbf{s}_k^* + \sigma^2 \mathbf{I} \tag{6}$$

and its properties are well documented [1]. Because of the angle-Doppler linear relationship in (5), in the narrowband case for a specific look direction, the adaptive space-time processor using (6) will null out clutter components induced along that direction thereby making target detection possible.

II. WIDBAND STAP PERFORMANCE

To obtain a similar understanding for the structure of the data and array output covariance matrix in the wideband case, assume that matched filtering and adaptive processing is employed in that case as well. Consider a wideband signal $f(t)$ with bandwidth B_o that is modulated by frequency ω_o to generate $f(t)e^{j\omega_o t}$ which acts as the transmit signal. When a wideband waveform is employed in the context of space time adaptive processing (STAP), the finite bandwidth dispersion across the antenna must be taken into account. To understand the bandwidth dispersion issues, let $e^{j\omega_o t}$ and $f(t)e^{j\omega_o t}$ refer to the transmit waveforms in the narrowband and wideband situation respectively across an N element array employing M pulses. Here (see Fig. 1)

$$f(t) \leftrightarrow F(\omega) = \begin{cases} F(\omega), & |\omega| \le B_o/2 \\ 0, & |\omega| > B_o/2 \end{cases}. \tag{7}$$

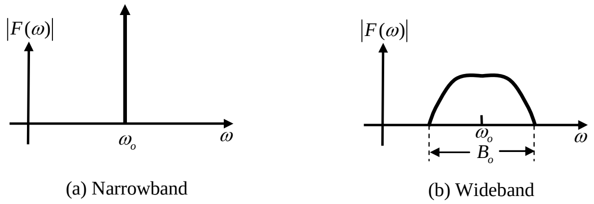

Fig. 1 Narrowband and width band transmit signals.

Let $y_1^{(1)}(t) = f(t)e^{j\omega_o t}$ represent the scattered return at the reference sensor due to the first pulse from a ground location at an azimuth angle θ_k for a specific range. In that case, the i^{th} sensor output (suppressing the noise component) is given by

$$y_1^{(i)}(t) = f\left(t-(i-1)\tau_1\right)e^{j\omega_o\left(t-(i-1)\tau_1\right)}, \quad i=1,\ 2,\ \cdots\ N \tag{8}$$

where

$$\tau_1 = \frac{d\sin\theta_k}{c} \tag{9}$$

represents the interelement time delay corresponding to azimuth angle θ_k. This gives the first pulse output across the array to be

$$\underline{y}_1(t) = \left[\ f(t)e^{j\omega_o t},\ \ \cdots\ f\left(t-(N-1)\tau_1\right)e^{j\omega_o\left(t-(N-1)\tau_1\right)}\right]^T. \tag{10}$$

Similarly, the received signal at the reference sensor due to the n^{th} pulse is given by

$$\begin{aligned} y_n^{(1)}(t) &= f\left(t-(n-1)\tau_2\right)e^{j\omega_o\left(t-(n-1)\tau_2\right)} \\ &= f\left(t-(n-1)\tau_2\right)e^{-j\pi(n-1)\omega_{d\,k}}\ e^{j\omega_o t} \end{aligned} \tag{11}$$

where ω_{d_k} is as defined in (5) and

$$\tau_2 = \frac{2VT\sin\theta_k}{c} \tag{12}$$

represents the interpulse delay for azimuth angle θ_k. After demodulation, the output at the i^{th} sensor is given by

$$\begin{aligned} z_n^{(i)}(t) = f\left(t-(n-1)\tau_2-(i-1)\tau_1\right)e^{-j\pi(n-1)\omega_{d\,k}}\ e^{-j(i-1)\tau_1}, \\ i=1,\ 2,\ \cdots N,\quad n=1,\ 2,\ \cdots\ M. \end{aligned} \tag{13}$$

Notice that the time-delayed version of the baseband waveform in the return signal is characteristic of the wideband situation. Using (11) - (12) with $\underline{z}_n(t),\ n=1,\ 2,\ \cdots\ M$ representing the array output vector for the 1^{st}, 2^{nd}, $\cdots\ M^{th}$ pulse, we get the space-time vector $\mathbf{z}(t)$ due to a single scatter to be [2] (details omitted)

$$\mathbf{z}(t) = \begin{bmatrix} \underline{z}_1(t) \\ \underline{z}_2(t) \\ \vdots \\ \underline{z}_M(t) \end{bmatrix} \tag{14}$$

where

$$\underline{z}_n(t) = \left[z_n^{(1)}(t),\ z_n^{(2)}(t),\ \cdots\ z_n^{(N)}(t)\right]^T. \tag{15}$$

This gives

$$\mathbf{z}(t) = \mathbf{f}_k(t)\circ\mathbf{s}(\theta_k,\ \omega_{d_k}) \tag{16}$$

where $\mathbf{s}(\theta_k,\ \omega_{d_k})$ is as defined in (2) - (5) and $\circ$ represents the element-wise (Schur-Hadamard) multiplication. Here $\mathbf{f}_k(t)$ represents an $MN\times 1$ transmit signal dependent vector whose $(iN+n)^{th}$ element is given by (see (13))

$$\begin{aligned} f\left(t-n\,\tau_2-i\,\tau_1\right),\quad i=0,1,2,\cdots N-1, \\ n=0,1,2,\cdots,M-1. \end{aligned} \tag{17}$$

Let

$$\mathbf{T}_k(\tau) = E\left\{\mathbf{f}_k(t)\mathbf{f}_k^*(t+\tau)\right\} > 0 \tag{18}$$

represent the covariance matrix associated with the return wideband signal vector $\mathbf{f}_k(t)$ in (16). We will assume that the actual return signal components in (17) resulting from random scatter modulations are stochastic in nature with wide sense stationary behavior, such that its power spectrum coincides with the original wideband transmit signal spectrum in Fig. 1 (b). This is a reasonable assumption, since the returns are inherently stochastic due to the physics of the problem, nevertheless their spectral content is assumed to be dictated by the transmit signal. As a result, the autocorrelation function $\mathbf{T}_k(\tau)$ in (18) is dictated by the inverse Fourier transform of the baseband version of the wideband signal power spectrum.

Extending the summation over all scatterers in (16), the array output covariance matrix in the fully wideband case takes the form

$$\mathbf{R}_z = E\left\{\mathbf{z}(t)\mathbf{z}^*(t)\right\} = \sum_k P_k\,\mathbf{T}_k\circ\mathbf{s}_k\mathbf{s}_k^* + \sigma^2\mathbf{I} \tag{19}$$

where $\mathbf{T}_k = \mathbf{T}_k(0)$. For example, a low pass power spectrum for the transmit signal gives

$$\mathbf{T}_k(m,\ n) = \operatorname{sinc} B_o\left((n_1-n_2)\tau_2(k)+(i_1-i_2)\tau_1(k)\right) \tag{20}$$

where n_1, n_2, i_1 and i_2 satisfy

$$m = i_1 N + n_1, \quad n = i_2 N + n_2 \ . \tag{21}$$

In the special case, such as when the azimuth spread generates only a small angular dispersion $\Delta\theta$ due to a strong main beam pattern, the $\mathbf{T}_k$ in (19) may be replaced by a positive definite matrix $\mathbf{T}$ that is valid for all k. In that case (19) reduces to

$$\mathbf{R}_z = \mathbf{T} \circ \mathbf{R}_x \tag{22}$$

where $\mathbf{R}_x$ represents the narrowband situation in (6). It is well known that even for moderate bandwidth the Schur-Hadamard operation in (22) results in spreading the eigenvalue spectrum of $\mathbf{R}_x$ thereby increasing the clutter degrees of freedom [1]. This is shown in Fig. 2 for a 14 sensor 16 pulse array with $CNR = 40\,dB$ and $\mathbf{T}_k$ as in (20).

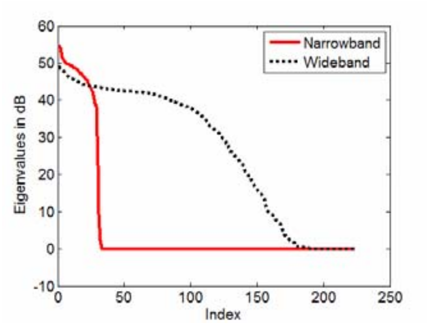

Fig. 2 Clutter eigen spectra for narrowband and wideband cases.

III. Wideband Analysis

To fully understand the implication of the Schur-Hadamard product operation in (16) - (19), let us consider a simplified version of (19), where the corresponding narrowband scatter set corresponds to a single scatter from θ_o; i.e.,

$$\mathbf{R}_x = P_o\, \mathbf{s}(\theta_o, \omega_{d_o}) \mathbf{s}^*(\theta_o, \omega_{d_o}) \tag{23}$$

and hence from (19)

$$\mathbf{R}_z = \mathbf{T}_o \circ \left(P_o\, \mathbf{s}(\theta_o, \omega_{d_o}) \mathbf{s}^*(\theta_o, \omega_{d_o}) \right) . \tag{24}$$

To make further progress, let

$$\mathbf{T}_o = \sum_{i=1}^{MN} \lambda_i\, \mathbf{e}_i\, \mathbf{e}_i^* \geq 0 \tag{25}$$

represent the eigen decomposition of $\mathbf{T}_o$ in (18). Substituting (25) into (24) we get

$$\mathbf{R}_z = \sum_{k=1}^{MN} P_k\, \tilde{\mathbf{s}}_k \tilde{\mathbf{s}}_k^* + \sigma^2 \mathbf{I} \tag{26}$$

where

$$P_k = P_o \lambda_k > 0 \tag{27}$$

and

$$\tilde{\mathbf{s}}_k = \mathbf{e}_k \circ \mathbf{s}(\theta_o, \omega_{d_o}) \ . \tag{28}$$

Observe that (26) represents a bunch of MN uncorrelated returns, all of them associated with the single scatter located along θ_o. Interestingly, $\tilde{\mathbf{s}}_k$ in (26) represents a spatio-temporally amplitude modulated steering vector associated with the Doppler frequency ω_{d_o} and location θ_o.

Let $\mathbf{d}_k$ represent the ordinary DFT vector associated with the eigenvector $\mathbf{e}_k$. The entries in $\mathbf{e}_k$ correspond to a double sampling period of τ_1 followed by τ_2. As a result, it can be shown that

$$\mathbf{e}_k = \sum_{n=1}^{MN} d_k(n) \left(\underline{b}\left(\frac{2\, j_n}{M}\right) \otimes \underline{a}\left(\frac{i_n\, c_o}{N}\right) \right) \tag{29}$$

where $d_k(n)$ represents the n^{th} entry of $\mathbf{d}_i$ and c_o is a normalization constant. Here i_n and j_n represent the unique solution to the equation $n = (j_n - 1)N + i_n$, $j_n = 1, 2, \cdots M$, $i_n = 1, 2, \cdots N$.

Using (29) in (28) we get the modified steering vectors in (26) - (28) to be

$$\begin{aligned} \tilde{\mathbf{s}}_k &= \sum_{n=1}^{MN} d_k(n) \left\{ \underline{b}\left(\frac{2\, j_n}{M}\right) \otimes \underline{a}\left(\frac{i_n\, c_o}{N}\right) \right\} \circ \left(\underline{b}\left(\omega_{d_o}\right) \otimes \underline{a}\left(\theta_o\right) \right) \\ &= \sum_{n=1}^{MN} d_k(n) \left\{ \underline{b}\left(\omega_{d_o} + \frac{2\, j_n}{M}\right) \otimes \underline{a}\left(\theta_o + \frac{i_n\, c_o}{N}\right) \right\} \\ &= \sum_{n=1}^{MN} d_k(n)\, \mathbf{s}(\theta_o + \frac{i_n\, c_o}{N}, \omega_{d_o} + \frac{2\, j_n}{M}) = \sum_{n=1}^{MN} d_k(n)\, \mathbf{s}(\theta_n, \omega_{d_n}) \end{aligned} \tag{30}$$

where

$$\theta_n = \theta_o + \frac{i_n\, c_o}{N}, \quad \omega_{d_n} = \omega_{d_o} + \frac{2\, j_n}{M} \ . \tag{31}$$

From (30) - (31), the amplitude modulated steering vector $\tilde{\mathbf{s}}_k$ in (26)-(28) represents a coherent sum of steering vectors originating from locations θ_n, $n = 1 \rightarrow MN$ with Doppler components ω_{d_n}, $n = 1 \rightarrow MN$ as in (31). Referring back to (26), for each scatter return, the effect of finite bandwidth is to introduce an apparent jittering effect both on angle and Doppler domains so that a bunch of uncorrelated returns are generated. Each such uncorrelated return contains a set of coherent returns with different directional and Doppler components as in (31). This is illustrated in Fig. 3. Observe that the vector $\tilde{\mathbf{s}}_k$ in (30) contains several coherent returns, and it *does not* correspond to any physical steering vector. As a result, the adaptive processor based on (26) will not be able to null out either the original return from location θ_o or any of the coherently combined vectors. From (26), the wideband data $\mathbf{z}(t)$ in (16) can be equivalently expressed as

$$\mathbf{z}(t) = \sum_{k=1}^{MN} \alpha_k \sum_{n=1}^{MN} d_i(n)\, \mathbf{s}(\theta_n, \omega_{d_n}) = \sum_{k=1}^{MN} \alpha_k \tilde{\mathbf{s}}_k \qquad (32)$$

and it represents MN uncorrelated bunches, each bunch containing MN coherent returns from various jittered locations around with θ_o.

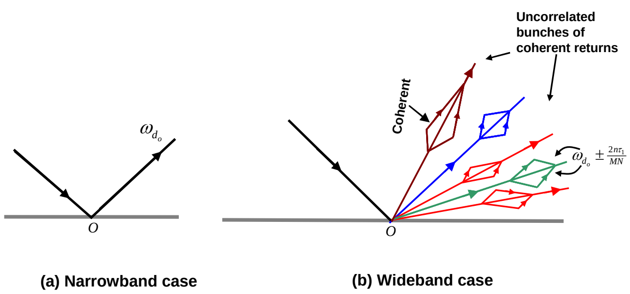

Fig. 3 Narrowband returns and effective wideband returns.

Fig. 4 shows the SINR loss of the adaptive processing with and without bandwidth dispersion. From there, the clutter null is wider due to the wideband operation nature of problem.

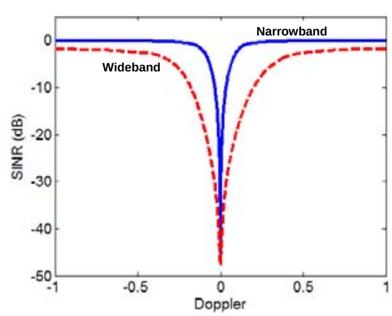

Fig. 4 Effect of wideband on clutter nulling performance.

III. Summary and Areas for Future Investigation

In summary, when traditional processing is employed in the wideband case a single scatterer appears to generate several isolated coherent bundles, thereby making clutter cancellation impossible. Thus, alternate processing schemes must be considered to fully resolve the wideband situation.

Presently, there are only two basic classes of techniques that have been proposed to remedy the wideband STAP clutter cancellation problem: Subband based methods or 3D STAP [3]-[4]. The subbanding approach, as the name implies, attempts to transform the wideband processing problem into a parallel set of narrowband 2D (angle-Doppler) STAP filters. Since a single 2D STAP processing thread is already a quite substantial processing burden, a bank of say L subband processors would represent an $L \times 100\%$ increase in processing burden!

The situation for 3D STAP is even worse. “3D” here refers to including the fast-time (i.e., reciprocal of receiver bandwidth) or equivalently instantaneous frequency domain. In other words, the dimensionality of the STAP problem is increased from NM to NML, where N is the number of spatial degrees-of-freedom (DOFs), M is the number of so-called “slow-time” or Doppler DOFs [1], and L is the number of fast-time or instantaneous DOFs. Since processing burdens are roughly on the order of $O(k^2) \rightarrow O(k^3)$, 3D STAP can result in an $L^2 \rightarrow L^3$-fold increase!

The above processing burden increases are in addition to the many other practical difficulties associated with implementing such adaptive filtering schemes, such as sufficient sample support for weights calculation [1] – a problem which is already acute for 2D STAP.

A practical framework for addressing the above issues is hierarchical processing in which an “energy preserving” lower resolution processing stage, to which 2D STAP could be applied, is followed by wideband processing only if a detection was obtained in the first stage. Even for the most stressing MTI applications, detections represent a very small fraction of all possible resolution cells—thus resulting in a substantially reduced wideband processing burden.

Aknowledgment

The research described herein is supported by the Air Force Research Laboratory (AFRL) Sensors Directorate, Radar Signal Processing Branch under USAF Contract FA8750-06-C-0117.

References

[1] J. R. Guerci, *Space-Time Adaptive Processing for Radar*, Artech House, Boston, 2003.

[2] T.C. Cheston and J. Frank, “Phase Array Radar Antenna”, *Radar Handbook*, Chapter 7, McGraw Hill, New York 1990.

[3] A. O. Steinhardt and N. B. Pulsone, “Subband STAP processing: the fifth generation”, *Proceedings of the 2000 IEEE Sensor Array and Multichannel Signal Processing Workshop*, pp. 1-6, March 16-17, Cambridge, MA, 2000.

[4] A. Hoffman and S. M. Kogon, “Subband STAP in wideband radar systems”, *Proceedings of the 2000 IEEE Sensor Array and Multichannel Signal Processing Workshop*, pp. 256-260, March 16-17, Cambridge, MA, 2000.